Observation of Large Kerr Nonlinearity at Low Light Intensities

Hoonsoo Kang and Yifu Zhu
Department of Physics, Florida International University, Miami, Florida 33199, USA
(Received 6 March 2003; published 26 August 2003)

We report an experimental observation of large Kerr nonlinearity with vanishing linear susceptibilities in coherently prepared four-level rubidium atoms. Quantum coherence and interference manifested by electromagnetically induced transparency suppress the linear susceptibilities and greatly enhance the nonlinear susceptibilities at low light intensities. The measured Kerr nonlinearity is comparable in magnitude to the linear dispersion in a simple two-level system and is several orders of magnitude greater than the Kerr nonlinearity of a conventional three-level scheme under similar conditions.

DOI: 10.1103/PhysRevLett.91.093601 PACS numbers: 42.50.Gy, 32.80.–t, 42.65.–k

Kerr nonlinearity corresponds to the dispersive part of third-order susceptibilities in an optical medium and has found many applications in nonlinear optics [1]. Recent studies have shown that Kerr nonlinearity can be used for quantum nondemolition measurements, quantum logic gates, quantum state teleportation, and nonlinear light control [2–5]. It is desirable to have large third-order nonlinear susceptibilities under conditions of low light powers and high sensitivities. This requires that the linear susceptibility should be as small as possible for all pump and signal fields in order to minimize absorption loss. However, these requirements are incompatible in conventional devices. To overcome this difficulty, Schmidt and Imamoglu proposed a scheme based on a four-level system with electromagnetically induced transparency (EIT) [6]. The EIT scheme is capable of producing greatly enhanced third-order susceptibilities and, at the same time, completely suppressing the linear susceptibilities. The absorptive part of the enhanced third-order nonlinearities may be used to study pure two-photon absorption and realize a quantum switch operating at few-photon levels [7,8]. The refractive part of the enhanced third-order nonlinearities, the Kerr nonlinearity, can be many orders of magnitude greater than that obtained in a conventional three-level scheme and may be used to obtain significant cross-phase modulation (XPM) at weak light intensities [6]. Recently, Matsko *et al.* showed that the efficient Kerr nonlinearity may be also obtained in a M-type multilevel system [9].

The EIT scheme for producing the large Kerr nonlinearity has attracted considerable attention due to its potential applications in quantum optics and quantum information science [10–14]. Here we report the experimental observation of the large Kerr nonlinearity in the four-level EIT scheme. Our experiments were done with cold ^{87}Rb atoms confined in a magneto-optical trap (MOT). We observed the Kerr nonlinearity at low light intensities with amplitudes comparable to those of the linear dispersion in a simple two-level system, which results in the XPM phase shifts several orders of magnitude greater than those of a conventional three-level scheme.

Consider the four-level EIT system as depicted in Fig. 1(a) [6]. A coupling laser driving the transition $|2\rangle$–$|3\rangle$ with Rabi frequency $2\Omega_c$ and a probe laser (frequency ω_p) driving the transition $|1\rangle$–$|3\rangle$ with Rabi frequency $2\Omega_p$ create the standard Λ-type EIT. A signal laser (frequency ω) drives the transition $|2\rangle$–$|4\rangle$ with Rabi frequency 2Ω. In the dressed-state picture, the signal laser induces the cross-phase modulation of the probe laser similar to that in a conventional three-level XPM scheme [Fig. 1(b)] [6]. The induced polarization at the probe frequency is $P(\omega_p) = \varepsilon_0 \chi(\omega_p) E(\omega_p)$, where the susceptibilities $\chi(\omega_p) = \chi^{(1)} + \chi^{(3)}|E(\omega)|^2 + \cdots$. Here $E(\omega_p)$ and $E(\omega)$ are the electric fields of the probe and the signal lasers, respectively. As shown in [6], when both the coupling laser detuning Δ_c and the probe laser detuning Δ_p are zero, EIT suppresses the linear susceptibility $\chi^{(1)}$ and greatly enhances the third-order susceptibility $\chi^{(3)}$. Under the EIT condition $\Omega_c \gg \Omega_p$ and $\Delta_c = \Delta_p = 0$, the nonlinear dispersion $\mathrm{Re}(\chi)$ and the total absorption loss $\mathrm{Im}(\chi)$ of the four-level system are [6,7]

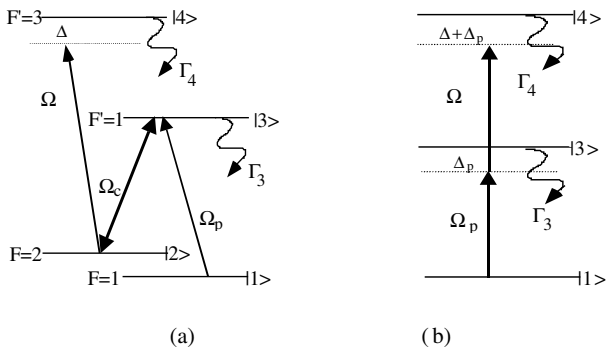

FIG. 1. (a) Four-level EIT scheme for the enhanced Kerr nonlinearity. (b) Conventional three-level XPM scheme. A signal laser induces XPM phase shifts of a probe laser. Γ_3 (Γ_4) is the spontaneous decay rate of the state $|3\rangle$ ($|4\rangle$).

 0031-9007/03/91(9)/093601(4)$20.00

$$\mathrm{Re}(\chi) = \frac{16K|\Omega|^2|\Omega_c|^2\Delta}{4(2|\Omega_c|^2 + \gamma_2\Gamma_3)^2\Delta^2 + (2|\Omega_c|^2\Gamma_4 + 2|\Omega|^2\Gamma_3 + \gamma_2\Gamma_3\Gamma_4)^2}, \tag{1a}$$

$$\mathrm{Im}(\chi) = K\frac{8|\Omega|^2(|\Omega_c|^2\Gamma_4 + |\Omega|^2\Gamma_3 + \gamma_2\Gamma_3\Gamma_4) + 2\gamma_2(2|\Omega_c|^2 + \gamma_2\Gamma_3)(\Gamma_4^2 + 4\Delta^2)}{4(2|\Omega_c|^2 + \gamma_2\Gamma_3)^2\Delta^2 + (2|\Omega_c|^2\Gamma_4 + 2|\Omega|^2\Gamma_3 + \gamma_2\Gamma_3\Gamma_4)^2}, \tag{1b}$$

where $K = N|\mu_{13}|^2/(3V\varepsilon_0\hbar)$. Δ is the frequency detuning of the signal laser, and γ_2 is the decay rate of the $|2\rangle$–$|1\rangle$ coherence. The first term in Eq. (1b) represents the nonlinear absorption while the second term represents the absorption loss due to decay of the $|2\rangle$–$|1\rangle$ coherence in the EIT system. The third-order nonlinearity is dominant when $\Omega_c > \Omega$. The nonlinear absorption coefficient is $\alpha = 2\pi\,\mathrm{Im}(\chi)/\lambda$ and the XPM phase shift is $\phi = \pi\ell\,\mathrm{Re}(\chi)/\lambda$ (λ is the probe wavelength and ℓ is the medium length). The figure of merit for the Kerr nonlinearity can be defined as $\eta = \phi/\alpha\ell$. In particular, Eq. (1) shows that, when $\gamma_2 \approx 0$ and $\Omega_c \sim \Omega$, $\mathrm{Re}(\chi) \approx 4K\Delta/[4\Delta^2 + (\Gamma_3 + \Gamma_4)^2]$ and $\mathrm{Im}(\chi) \approx 2K(\Gamma_3 + \Gamma_4)/[4\Delta^2 + (\Gamma_3 + \Gamma_4)^2]$. The figure of merit is then $\eta = \Delta/(\Gamma_3 + \Gamma_4)$, which increases linearly with Δ. For comparison, consider the weak-field, linear susceptibility $\chi^{(1)}$ in a simple two-level system, which is given by $\mathrm{Re}[\chi^{(1)}) = 4K\Delta/(4\Delta^2 + \Gamma^2]$ and $\mathrm{Im}[\chi^{(1)}) = 2K\Gamma/(4\Delta^2 + \Gamma^2]$ (Γ is the decay rate of the excited state). The two-level linear susceptibility sets the fundamental upper limit for all orders of nonlinear susceptibilities at low light intensities. The above results show that $\chi^{(3)}|E(\omega)|^2$ in the four-level EIT scheme may behave similar to the $\chi^{(1)}$ linear susceptibility in the simple two-level system with comparable amplitudes. Therefore, large XPM phase shifts can be obtained in the EIT scheme at very weak light intensities (with the EIT condition $|\Omega_c|^2 > \gamma_2\Gamma_3$ and $\Omega_c \ll \Gamma_3$ if $\gamma_2 \sim 0$). For our experiments on cold Rb atoms, $\gamma_2 \sim 10^4\ \mathrm{s}^{-1}$ and the lower limit of the coupling Ω_c is set by the laser linewidth ($\sim$1 MHz). We can choose $\Omega_c \sim \Omega < \Gamma_3$ (below the saturation levels), and obtain the EIT enhanced Kerr nonlinearity with the amplitudes approaching that of the linear susceptibility of the simple two-level system.

For comparison with the conventional XPM scheme in a three-level system [Fig. 1(b)] [6], we calculate the susceptibilities for the probe transition $|1\rangle$–$|3\rangle$ and derive the XPM figure of merit for the three-level scheme,

$$\eta' = \frac{4|\Omega|^2(\Delta + \Delta_p)}{(4|\Omega|^2 + \Gamma_3\Gamma_4)\Gamma_4 + 4\Gamma_3(\Delta + \Delta_p)^2}, \tag{2}$$

where Δ (Δ_p) is the signal (probe) laser detuning. Because of the absorption loss in the three-level scheme at low light intensities (due to the dominant linear susceptibility $\chi^{(1)}$), large frequency detunings Δ and Δ_p are needed, which then require large signal laser intensities in order to achieve a reasonably large η' value. For a numerical comparison between the EIT scheme and the three-level scheme, consider $\Omega_c = \Omega = 0.3\Gamma_3$, $\Delta = 10\Gamma_3$, and $\Gamma_3 \approx \Gamma_4$, we obtain $\eta \approx 5$ for the EIT scheme. For the three-level scheme with the equal absorption loss under similar conditions ($\Omega = 0.3\Gamma_3$, $\Delta = \Delta_p = 10\Gamma_3$), the figure of merit $\eta' \approx 0.0022$. The EIT enhancement factor is $\sim$2000. The enhancement factor increases rapidly versus the increasing frequency detuning Δ and can be as large as 10^9 in some practical considerations [6].

In our experiment, a tapered-amplifier diode laser (TA-100, Tuioptics) with output power of $\sim$300 mW is used as the cooling and trapping laser. An extended-cavity diode laser with an output power of $\sim$30 mW is used as the repump laser. The diameter of the trapping laser beams and the repumping laser beam is $\sim$2.5 cm. The trapped ^{87}Rb atom cloud is $\sim$3 mm in diameter and contains $\sim 10^9$ atoms. A simplified experimental scheme is depicted in Fig. 2. The coupling field driving the $D_1F = 2$–$F' = 1$ transition is provided by a third extended-cavity diode laser with a beam diameter $\sim$5 mm and output power $\sim$20 mW. A fourth extended-cavity diode laser with a beam diameter $\sim$5 mm is used as the signal laser that drives the $D_2F = 2$–$F' = 3$ transition. The probe laser connecting the $D_1F = 1$–$F' = 1$ transition is provided by a fifth extended-cavity diode laser with a beam diameter $\sim$1 mm. The laser intensities are varied by neutral density filters. The linewidth of the extended-cavity diode lasers is $\sim$1 MHz. The probe laser, the coupling laser, and the signal laser are overlapped with the trapped Rb cloud. The probe laser and the signal laser

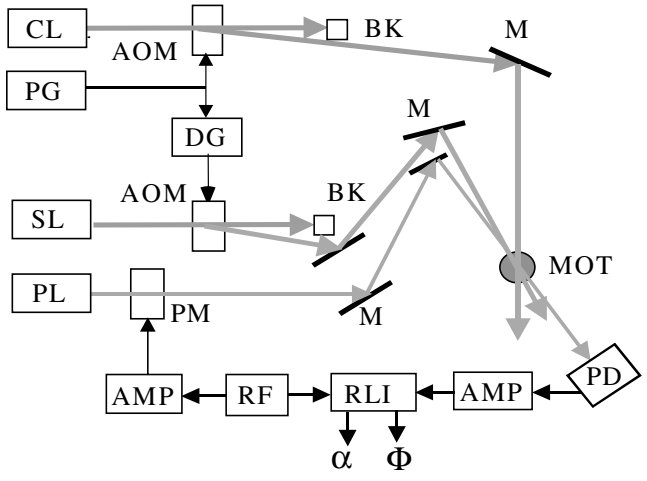

FIG. 2. Schematic diagram of the experimental setup. CL: coupling laser; SL: signal laser; PL: probe laser; PG: pulse generator; DG: delay generator; AOM: acousto-optic modulator; M: mirror; BK: beam blocker; PD: fast photodetector; PM: phase modulator; RF: rf function generator; AMP: rf amplifier; RLI: rf lock-in amplifier.

propagating at an angle of ~4° relative to each other have a spatial angle of ~45° relative to the propagating direction of the coupling laser. The noncollinear excitation scheme minimizes the effects of the nonlinear wave mixing on the response of the probe laser (including the low frequency transition between the states $|1\rangle$ and $|2\rangle$) since it does not meet the phase matching condition [11].

In order to measure simultaneously the phase shift and the amplitude attenuation experienced by the probe laser, the frequency modulation (FM) spectroscopic technique is used [15]. The probe laser is phase modulated at 100 MHz and contains three frequency components at ω_p and $\omega_p \pm 2\pi\nu$ ($\nu = 100$ MHz). In the experiment, one of the sideband frequencies of the probe laser, $\omega_p + 2\pi\nu$, is locked to the $D_1F = 1 \rightarrow F' = 1$ transition frequency. After transmission through the MOT, the probe field is given by $E(\omega_p) = 1/2\tilde{E}(\omega_p) + \text{c.c.}$ with $\tilde{E}[\omega_p) = E_0(e^{i\omega_p t} + M/2e^{-\alpha\ell/2 - i\phi}e^{i(\omega_p + 2\pi\nu)t} - M/2e^{i(\omega_p - 2\pi\nu)t}]$ ($M \sim 0.3$ is the phase modulation index). Because of the large frequency detuning of the carrier (ω_p) and the lower sideband ($\omega_p - 2\pi\nu$) from the probe transition (100 and 200 MHz, respectively), the absorption and dispersion of the carrier and the lower sideband are negligible. The transmitted probe beam is collected by a fast photodiode and the detector output signal is given by $S = \eta|E(\omega_p)|^2$ (η is the detector efficiency). The photodiode signal is then amplified and sent to a rf lock-in amplifier (SR844, Stanford Research Systems). The rf lock-in amplifier mixes the signal with the 100 MHz local oscillator and provides simultaneously two dc output signals, one in-phase and the other quadrature of the detector signal (demodulated at 100 MHz). The in-phase signal is given by $S_i = aM|E_0|^2e^{-\alpha\ell/2}\cos(\phi + \delta)$ and the quadrature signal is given by $S_q = aM|E_0|^2e^{-\alpha\ell/2}\sin(\phi + \delta)$ (δ is a phase factor and a is an efficiency constant). With appropriate adjustment of the reference phase of the rf lock-in amplifier, δ can be set to ~0. The two signals S_q and S_i are recorded simultaneously by a digital oscilloscope (Tektronix TDS460), which yields the nonlinear absorption coefficient α and the XPM phase shift ϕ.

The experiment is run in a sequential mode with a repetition rate of 5 Hz. All lasers except the probe laser are turned on and off by acousto-optic modulators (AOM) according to the time sequence described below. For each period of 200 ms, ~192 ms is used for cooling and trapping of the Rb atoms, during which the trap laser and the repump laser are turned on by two separate AOMs while the coupling laser and the signal laser are off. The weak, continuous probe laser does not disturb the MOT. The coupling laser frequency is locked on the $D_1F = 2 \rightarrow F' = 1$ transition and one of the FM sidebands of the probe laser is locked on the $D_1F = 1 \rightarrow F' = 1$ transition. The time for the measuring the probe transmission signals (S_q and S_i) lasts ~8 ms, during which the trap laser and the repump laser are turned off, and the coupling laser and the signal laser are turned on by two additional AOMs. 20 μs after the coupling laser and the signal laser are turned on, the signal laser frequency is scanned across the $D_2F = 2 \rightarrow F' = 3$ transition in ~5 ms and the probe signals S_q and S_i are recorded. Since the laser pulse durations are much greater than the atomic decay times $1/\Gamma_3$ (30 ns) and $1/\Gamma_4$ (27 ns), the measurements are carried out essentially in the steady-state regime.

Figure 3 shows the measured quadrature signal S_q [3(a1), 3(a2), and 3(a3)] and the in-phase signal S_i [3(b1), 3(b2), and 3(b3)] versus the signal laser detuning Δ, while the coupling laser and the upper sideband of the FM modulated probe laser are locked on the respective transitions ($\Delta_c = \Delta_p = 0$). The spectra in Fig. 3 are observed only when the three lasers are present simultaneously, which suggests that the spectra arise from the nonlinear optical processes. The experimental data are plotted in solid lines while the dotted lines are the numerical calculations of the Rb four-level system [Fig. 1(a)]. The measurements of Fig. 3 were taken with $\Omega_c \approx 2$ MHz and $\Omega_p \approx 0.1$ MHz (determined from the measured EIT spectrum without the signal laser). Similar results were also observed with other Ω_c values. Since the EIT suppresses the linear susceptibility, the quadrature and the in-phase signals of the probe laser give the direct measure of the nonlinear susceptibilities. These measurements show that the observed nonlinear susceptibility behaves similar to the linear susceptibility of the simple two-level system. From separate measurements of the absorption spectrum of the probe laser under identical conditions but without FM, we measure directly the percentage attenuations of the probe laser from the nonlinear absorption loss, from which we calculate the absorption coefficient $\alpha\ell$. For Figs. 3(b1), 3(b2), and 3(b3), the derived peak values of $\alpha\ell \approx 0.15$, 0.28, and 0.52,

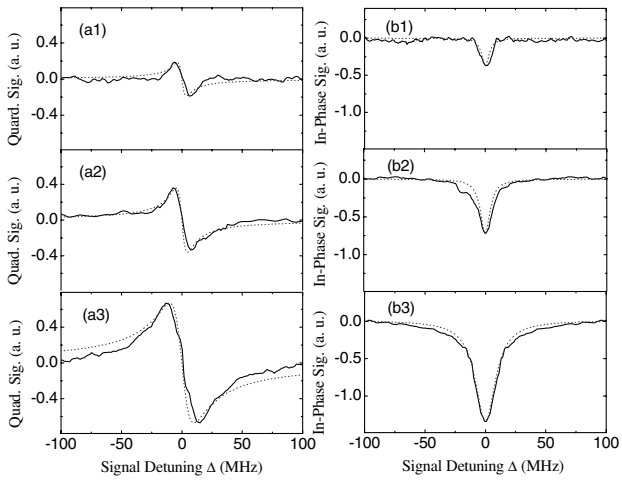

FIG. 3. Measured quadrature signals [(a1)–(a3)] and in-phase signals [(b1)–(b3)] versus the signal detuning Δ while $\Delta_c = \Delta_p = 0$. The solid (dotted) lines are the experimental (theoretical) results. The fitting parameters are $\gamma_2 = 0.01$ MHz, $\Omega_c = 2$ MHz, $\Omega_p = 0.1$ MHz, and $\Omega = 1$, 1.7, and 3 MHz, respectively (from the top to the bottom).

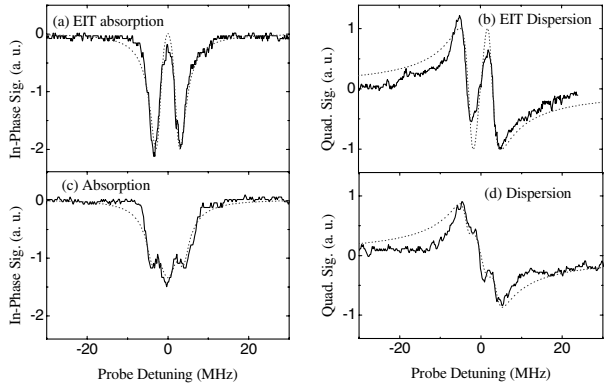

FIG. 4. Measured probe absorption [(a) and (c)] and probe dispersion [(b) and (d)] versus the probe detuning Δ_p while $\Delta_c = \Delta = 0$. The solid (dotted) lines represent the experimental data (the theoretical calculations). (a) and (b) show the EIT spectra of the absorption and dispersion (the signal laser is turned off). (c) and (d) show the probe spectra with the signal laser present. The fitting parameters are $\gamma_2 = 0.01$ MHz, $\Omega_c = 3$ MHz, $\Omega_p = 0.1$ MHz, and $\Omega = 3$ MHz.

respectively, which are then used to determine the XPM phase shifts ϕ. The peak XPM phase shifts from the measured quadrature signals in Figs. 3(a1), 3(a2), and 3(a3) are calculated to be about 2.1°, 4.0°, and 7.5°, respectively, which are about 19%, 36%, and 67% of the phase shift from the linear dispersion experienced by a weak probe laser in the two-level system (with $\Gamma = \Gamma_3$). As discussed previously, these values are several orders of magnitude greater than that of the conventional three-level Kerr nonlinearity under similar conditions.

To reveal how the nonlinear susceptibilities of the four-level system vary vs the probe laser frequency, we also measured the probe dispersion and the probe absorption versus the probe detuning Δp while the coupling laser and the signal laser are locked to their respective transitions ($\Delta = \Delta_c = 0$). Figures 4(a) and 4(b) plot the measured spectra of the EIT dispersion and EIT absorption without the signal laser ($\Omega = 0$), respectively, which show the familiar transparent EIT window in the absorption and the steep slope of the normal dispersion centered at $\Delta p = 0$. When the signal laser is present, the transparent window is replaced by an absorption peak representing the EIT enhanced third-order nonlinear absorption and the corresponding dispersion becomes anomalous near $\Delta p = 0$ as shown in Figs. 4(c) and 4(d). We observed that the amplitudes of the absorption and dispersion at $\Delta p = 0$ increase (decrease) as the signal laser intensity increases (decreases), consistent with the measurements shown in Fig. 3.

The large enhancement of the nonlinearity in the four-level EIT system may lead to single-photon devices in nonlinear optics [7,11]. In the ideal limit [7], a signal light pulse with a single photon in a 1 μs duration and focused to a spot size of a half wavelength (at 780 nm) has an intensity ~ 0.2 mW/cm^2, which corresponds to a signal field $\Omega \sim 1$ MHz here. This shows that, although our experiments are not carried out with single photons, the large XPM shifts are observed near the possible single-photon intensity levels for the signal laser and the probe laser. Further refinement of the experimental setup and the tight focus of the signal and the probe laser beams may render it possible to study the four-level EIT system with single photons.

In conclusion, we have observed the EIT enhanced Kerr nonlinearity with vanishing linear susceptibilities at low light intensities in a four-level EIT scheme. The resonantly enhanced Kerr nonlinearity behaves similar to the linear susceptibility in a weak-field driven two-level system. The observed XPM phase shifts are comparable in magnitudes with the phase shift of the linear dispersion in the two-level system. The experimental measurements agree with the theoretical calculations, and the Kerr nonlinearities derived from the measurements are several orders of magnitude greater than those of a conventional three-level XPM scheme. It will be interesting to explore the EIT enhanced Kerr nonlinearity for possible applications in quantum nonlinear optics and quantum measurements.

This work is supported by the National Science Foundation and the office of Naval Research.

[1] Y. R. Shen, *The Principles of Nonlinear Optics* (Wiley, New York, 1984).
[2] J. P. Poizat and P. Grangier, Phys. Rev. Lett. **70**, 271 (1993).
[3] Q. A. Turchette, C. J. Hood, W. Lange, H. Mabuchi, and H. J. Kimble, Phys. Rev. Lett. **75**, 4710 (1995).
[4] S. Rebic, S. M. Tan, A. S. Parkins, and D. F. Walls, J. Opt. B **1**, 490 (1999).
[5] H. Wang, D. Goorskey, and M. Xiao, Opt. Lett. **27**, 1354 (2002).
[6] H. Schmidt and A. Imamoglu, Opt. Lett. **21**, 1936 (1996); **23**, 1007 (1997).
[7] S. E. Harris and Y. Yamamoto, Phys. Rev. Lett. **81**, 3611 (1998).
[8] M. Yan, E. Rickey, and Y. Zhu, Opt. Lett. **26**, 548 (2001); Phys. Rev. A **64**, 041801 (2001).
[9] A. B. Matsko, I. Novikova, G. R. Welch, and M. S. Zubairy, Opt. Lett. **28**, 96 (2003).
[10] D. Vitali, M. Fortunato, and P. Tombesi, Phys. Rev. Lett. **85**, 445 (2000).
[11] S. E. Harris and L.V. Hau, Phys. Rev. Lett. **82**, 4611 (1999).
[12] M. D. Lukin and A. Imamoglu, Nature (London) **413**, 273 (2001).
[13] J. Clausen, L. Knoll L, and D. G. Welsch, J. Opt. B **4**, 155 (2002).
[14] A. Andre and M. D. Lukin, Phys. Rev. Lett. **89**, 143602 (2002).
[15] G. C. Bjorklund, Opt. Lett. **5**, 15 (1980).